Received on (10-10-2022) Accepted on (28-03-2023)

New Equations for Rate of Energy Dissipation of a Stepped Spillway with Slope less than Critical and Specific Step Height

Okechukwu Ozueigbo[1*] and J. C. Agunwamba[2]
[1, 2] Department of Civil Engineering, University of Nigeria, Nsukka
[1*]Corresponding author mail address: ozueigbo.okechukwu.pg78995@unn.edu.ng
https://doi.org/10.33976/JERT.10.2/2023/2

Abstract—Stepped spillways disperse energy in floodwater by utilizing their stepping nature. Several researchers investigated the hydraulic and geometric relationships of the stepped spillway with a dam slope above 26.6º, which resulted in energy dissipation. But a few studied stepped spillways with a dam slope of 26.6º with a step height of 0.61 m. This move led to a lack of knowledge and rules for the designers of stepped spillways with slope of 26.6º and a step height of 0.61 m. The authors reviewed the researchers' publications on horizontal stepped spillways with dam slopes of 26.6º with step height of 0.61 m conducted in transition and skimming flows in large-size facilities with phase-detection intrusive probes. They retrieved data sets from them, which they took into account to create two novel equations for energy dissipation in stepped spillways: one for nappe flow and one for skimming flow. The results showed that the measured data sets compared well with the data sets calculated from the two empirical models.

Keywords— Stepped Spillway, Energy Dissipation, Nappe Flow, Skimming Flow.

1 Introduction

In high velocity free-surface turbulent flows, large quantities of air bubbles/pockets move across the air-water interface being entrapped (air entrainment) in the water current and then are carried away within the flowing fluid and, eventually, exchanged back to the air flowing above the free-surface (Halbronn et al., 1953; Jevdjevich and Levin, 1953) [1, 2] . The resulting air-water flow, or self-aerated flow, is a mixture of air and water consisting of both air packets within water and water droplets surrounded by air (Chanson, 1997) [3].

Aerated flows are used in a variety of applications including chemical, civil, environmental, mechanical, mining, nuclear, and water engineering (Rao and Kobus, 1974) [4].

.Aeration is a major feature of stepped spillway flows that is important for re-oxygenation applications such as waste water treatment, chemical applications, and rivers under environmental stress. They range in size from extremely little to quite huge. Self-aerated flows are frequently observed in water and environmental systems, such as mountain streams, storm waterways, culverts, dropshafts, spillway chutes, tidal channels, and stilling basins, where aeration is largely uncontrolled (Wood, 1991) [5], and such flows are also relevant to water quality, sediment transport, ecological sustainability, and, ultimately, environmental integrated assessment within such systems. Physical modeling is used to examine aerated flows experimentally.

Physical models for such experimental studies must be created with accuracy. Alternatively, size effects may have an impact on extrapolating experimental results to full-scale prototype structures (Kobus, 1984) [6]. Aerated flows are usually investigated using a Froude similitude; however the dynamic similitude in a geometrically comparable model incorporates extra dimensionless parameters. Shear flows are governed by viscous effects, whereas surface tension forces drive the mechanisms of bubble breakdown and coalescence (Chanson and Gualtieri, 2008) [7]. As a result, dynamic similitude in aerated flow demands that the Froude, Reynolds, and Morton values in the prototype and its model be equal. Yet, unless working at full-scale, this is hard to execute using geometrically identical models.

A Froude and Morton similitude can be implemented in the prototype and in the laboratory using the same fluids, namely air and water, but the model Reynolds number cannot be as great as in the prototype, resulting in viscous-scale effects in small-size models (Rao and Kobus, 1974; Wood, 1985; Chanson, 2009; Ozueigbo and Agunwamba, 2022) [4, 8 - 10].

.

Turbulence near the air-water interface drives the exchange of air across the air-water contact. When the turbulent shear stress exceeds the surface tension force per unit area opposing interfacial breakdown, free-surface breakup and air entrainment occur (Hino, 1961; Ervine and Falvey, 1987) [11, 12]. When some air is entrained inside the majority of the flow, air pockets break up when the tangential shear stress exceeds the capillary force per unit area (Chanson, 2009) [13].

As bubbles and droplets are advected by the flow, particle collisions may cause them to coalesce, and air detrainment

due to buoyancy occurs. Bubble clustering may occur as a result of the intricate interactions between entrained air and turbulence.

A bubble cluster is described as a group of two or more bubbles separated from the other bubbles before and after the cluster. Previous research has shown that clustering analysis can provide some useful information about the interplay between turbulence and bubbly flow (Gualtieri and Chanson 2010, 2013; Wang et al., 2015a) [14 - 16].

The use of typical mono-phase flow instrumentation is not feasible due to the three-dimensional character of high-velocity air-water flows with multiple air-water contacts.

In stepped spillways, phase-detection intrusive probes are frequently used, and trials have been effective with optical fiber probes [17], conductivity probes [18 – 21], air probes, and a back flushing Pitot-Static tube [22].

Intrusive probes with phase detection can measure characteristic air-water flow properties such as void fraction, bubble count rate, and interfacial velocity, as well as characteristic aeration parameters such as the mean air concentration C_{mean}: where Y_{90} is the characteristic flow depth and C = 0.9.
The depth averaged characteristic void fraction metric repre-

$$C_{mean} = \frac{1}{Y_{90}} \times \int_0^{Y_{90}} C \times dy \qquad (1)$$

senting aeration inside a cross-section is the mean air concentration C_{mean}.

The basis of the conductivity probe is the difference in resistance between air and water, which generates an immediate voltage signal. The time averaged local air concentration or void fraction C, the number of air-to-water (or water-to-air) voltage shifts described as bubble count rate F, and the air bubble and water droplet chord sizes can all be calculated from a single sensor's signal using a threshold technique.

The cross-correlation analysis of the data from a double-tip conductivity probe with longitudinal spacing between the two probe sensors leads to the local time-averaged interfacial velocity V. [23] and [24] have more information on signal processing techniques.

2 INSTRUMENTATION AND EXPERIMENT PROGRAM

The air-water flow experiments were carried out using air probes, backup flushing Pitot - static tubes, and Point Gages at the step edges of Steps 1, 4, 8, 12, 16, and 20. VHS videotapes and 35 mm prints were used to obtain visual documentation.

The experimental program was designed to assess the hydraulic properties of flow through a simulated roller compacted concrete (RCC) stepped spillway under near-prototype circumstances.

The experimental facilities were built on a large scale to reduce viscous scale effects on microscopic air-water flow processes in high-velocity free-surface flows [25]. A water supply pipeline, baffled head box, entrance/transition, chute, stilling basin, and outlet works compose the test facility.

The concrete chute is roughly 34.0 m long, 3.0 m wide, and 1.5 m deep, with a slope of 1:2 (vertical: horizontal) and a total height of 15 m. The width of the chute was reduced to 1.2 m for the current study by employing a dividing wall (Figure 1) In addition; flat-lashboards were placed on the walls of the test portion of the chute, extending the depth to 2.1 m, providing additional freeboard. Plexiglass windows, 1.2 m by 1.2 m were installed at five locations in the dividing wall to provide observation of flow in the chute [25].

Figure 1: Experimental Facility

The stepped spillway was made up of twenty-five horizontal steps with a step height of 0.61 m and a step length of 1.22 m, allowing the 1: 2 (vertical, horizontal) slope to be maintained at the outdoor testing facility located at the Colorado State University Engineering Research Center, about four miles west of the main Colorado State University campus (Figure 2).

The air probe and back flushing Pitot – static tube were mounted on a Point Gage and carriage system for collecting data at the various stations (Figure 3). The manually operated carriage system allowed for two degrees of freedom with the movement along the length of the spillway parallel to the floor and latertal movement within the width of the spillway. The

remotely operated motorized point gage allowed for vertical movement of the instruction perpendicular to the floor of the spillway to obtain dara profile within the flow. All the profiles were taken along the centerline of the flume normal to the spillway floor (Figure 3).

Figure 2: Stepped Spillway, h = 0.61m

Figure 3: Carriage and Point Gage system with Instrume

Experimental flow conditions

Despite the fact that the current work concentrated on the skimming flow regime, preliminary experiments revealed that a nappe flow occurred when $d_c/h = 0.46$. At $d_c//h = 0.73$, a transition flow was seen, while for $d_c/h > 0.73$, skimming flows were observed.

The variations in flow regimes were consistent with the data in the literature (Chanson 2001, Chanson and Toombes 2004) [26, 27]. The developing flow measurements in this study were concentrated on the skimming flow regime (dc/h > 0.73).

Table 1 summarizes the experimental flow conditions and compares them to previous extensive experimental research.

Table 1: Summary of Experimental Flow Conditions

Flow Observations

Reference	θ	Step geometry	Flow conditions	Instrumentation	Comments
Present study	26.6 degree	Flat steps, h = 0.61 m, l = 1.22 m	dc/h = 0.46 (nappe), 0.46 < dc/h < 0.73 (Transition), dc/h ≥ 0.73 (skimming)	Air probe, backing flushing Pitot-static tube, Point Gage, Videotapes on VHF format 35 mm prints	25 Steps, W = 1.2 m

Flow conditions were observed for each test series across a variety of discharges. The flow at the overtopping crest and along the spillway length was documented using videotape recordings and still pictures. Flow conditions were watched

and recorded using five plexiglass windows installed along the spillway's sidewall.

It was observed in this study that Nappe flow regime occurred for unit discharges below 0.46 m^2/s, Transition flow regime occurred for unit discharges between flows between 0.46 m^2/s and 0.93 m^2/s, and skimming flow regime for unit discharges above 0.93 m^2/s

Figure 4: Transition flow, h =0.61 m, Q = 1.1 m^3/s

Figure 5: Transition Flow Regime, h = 0.61 m, Q = 1.1m^3/s (d_c/h = 0.73)

Figure 6: Skimming flow, h =0.61 m, Q = 2.8 m3/s

Figure 7: Skimming flow, h =0.61 m, Q = 2.8 m^3/s (d_c/h = 1.35)

3 ENERGY DISSIPATION

Energy dissipation was measured at the edges of Steps 1, 4, 8, 12, 16, and 20 of the flat horizontal stepped spillway lay-outs. Figure 8 depicts common distributions of the energy losses.

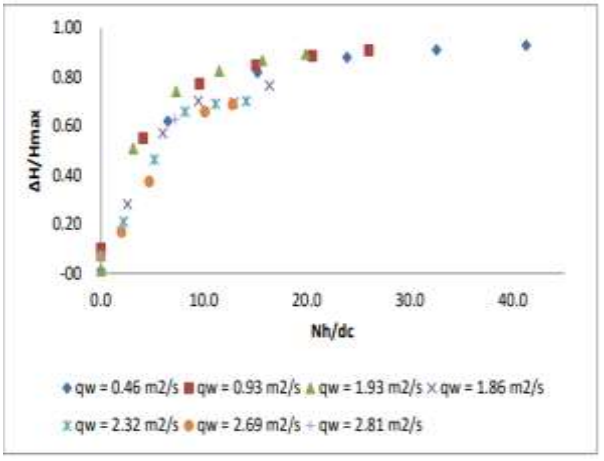

Figure 8: Energy dissipation rate on stepped spillways with embankment slope of 26.6o.

The current findings agreed with prior experimental air-water flow research [18 - 21]. Eq 2 was used to compute the rates of energy dissipation in Steps 1, 4, 8, 12, 16, and 20 for Q = 0.6 $m^3/2$ and 1.1 m^3/s.

(2)

$$\frac{\Delta H}{H_{max}} = 1 - \left\{ \frac{0.54\left(\frac{d_c}{h}\right)^{0.275} + \frac{3.43}{2}\left(\frac{d_c}{h}\right)^{-0.55}}{\frac{H_{dam}}{d_c} + \frac{3}{2}} \right\}$$

where H_{dam} is the dam height, d_c is the critical flow depth, and h is the step height.

While the rates at Steps 1, 4, 8, 12, 16, and 20 for Q = 1.7 m^3/s, 2.3 m^3/s, 2.8 m^3/s, 3.3 m^3/s, and 3.4 m^3/s were calculated based upon the upstream total head

$$H_{max} = H_{dam} + 1.5d_c \quad (3)$$

$$\Delta H = H_{max} - H_{res} \quad (4)$$

where H_{res} is estimated as

$$H_{res} = d\cos\theta + \frac{U_w^2}{2g} \quad (5)$$

$$d = \int_0^{Y_{90}} (1 - C)dy \quad (6)$$

where d denotes the equivalent clear water flow depth, U_w denotes the flow velocity ($U_w = q_w/d$), C is the void fraction, and Y_{90} denotes the characteristic elevation where C = 0.90.

Formulation of the Model

The authors used Figure 3 along with Eq (7) to formulate Eq (8) and Eq (9).

Where
ΔH/Hmax is the energy loss ratio,

$$\frac{\Delta H}{H_{max}} = \left[\alpha_o \frac{Nh}{d_c}\right]^{\alpha_1} N^{\alpha_2} \quad (7)$$

Hmax is the maximum available height,
N is the number of spillway steps,
h is the height of the spillway steps,
θ is the spillway channel slope.
ΔH is head loss,
d_c = critical water depth (m),
α_o, = constant,
α_1 and α_2 = coefficients

Model Calibration

They divided the measured data sets into two parts. They used one portion and multiple regression analysis to calibrate expression (7). The calibration yielded the values of constant α_o with the coefficients α_1, and α_2, which were then substituted in the expression to give the developed models in Eq (8) and Eq (9).

Model Verification

The authors used the remaining data sets, known as verification data sets, to evaluate the models' performance (interpolation).

If the model describes verification data well, then the model describes the real system and this is known the interpolation aspect [28].

4. RESULTS AND DISCUSSION

Developed model for the nappe/transition flow regime

$$\frac{\Delta H}{H_{max}} = \left[0.01\frac{Nh}{d_c}\right]^{0.19} N^{0.10} \quad (8)$$

Eq 8 is valid for a stepped spillway with a channel slope, $\boldsymbol{\theta}$ = 26.6º, step height, h = 0.61 m, number of steps, N not more 20, d_c/h not more than 0.73, and Nh/d_c not more than 27.0. The predicted data sets calculated with Eq (8) compared well with the measured data sets with the Pearson correlation of 0.99 (Figures 9 and 10).

Developed model for the skimming flow regime

The predicted data sets calculated with Eq (9) compared well with the measured data sets with the Pearson correlations

$$\frac{\Delta H}{H_{max}} = \left[0.35\frac{Nh}{d_c}\right]^{1.38} N^{-0.82} \quad (9)$$

of between 0.97 and 0.99 (Figures 11 to 15).

Eq 9 is valid for a stepped spillway with a channel slope, $\boldsymbol{\theta}$ = 26.6º, step height, h = 0.61 m, number of steps, N not more 20, d_c/h between 0.73 and 1.53, and Nh/d_c not more than 20.0.

In order to explore the impacts of discharge on energy dissipation in the skimming flow regime, Nh/d_c is given as a function of the dimensionless energy dissipation in Figures 9 through 15.

Energy losses for a given discharge rise progressively with an increasing dam height, which is consistent with [27].

For all the measured data sets, the dimensionless energy dissipation rates distribution compared well with Eq (8) for nappe flow and with Eq (9) for skimming flow.

In Figures 9 through 15, the measured data sets in the nappe flow and skimming flow compared well with developed data sets from Eq (8) and Eq (9) with Pearson Correlation of 0.99 for nappe flow and between 0.97 and 0.99 for skimming flow.

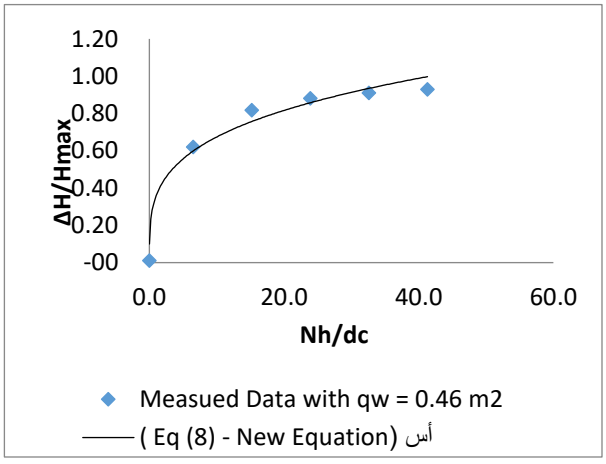

Figurre 9: ΔH/Hmax as a function of Nh/dc for qw = 0.46 m^2/s.

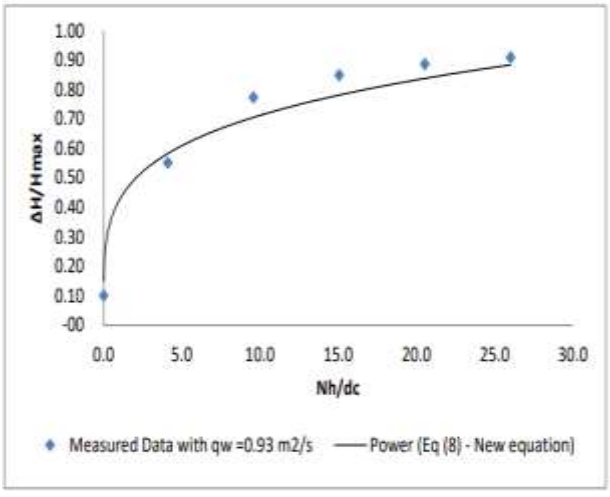

Figurre 10: ΔH/Hmax as a function of Nh/dc for qw = 0.93 m^2/s.

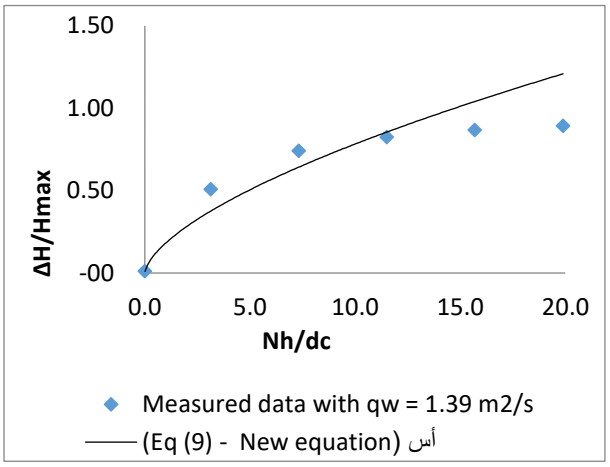

Figurre 11: ΔH/Hmax as a function of Nh/dc for qw = 1.39 m^2/s.

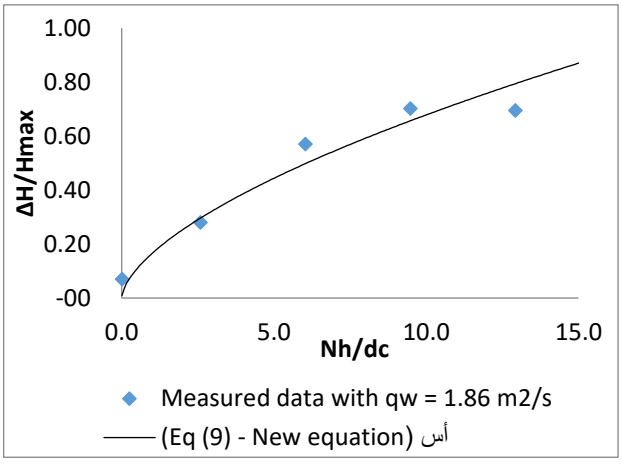

Figurre 12: ΔH/Hmax as a function of Nh/dc for qw = 1.86 m^2/s.

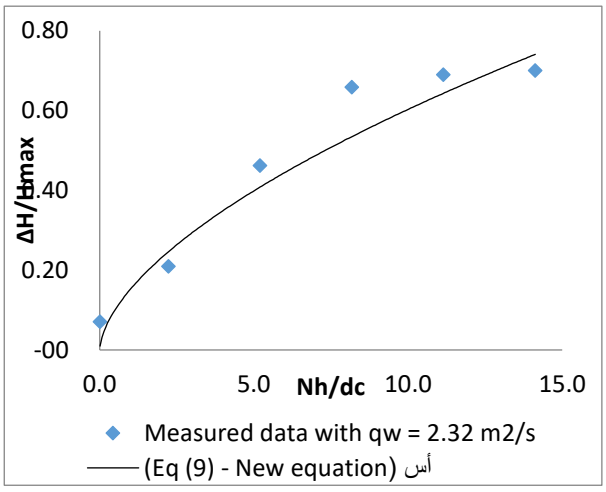

Figurre 13: ΔH/Hmax as a function of Nh/dc for qw = 2.32 m^2/s.

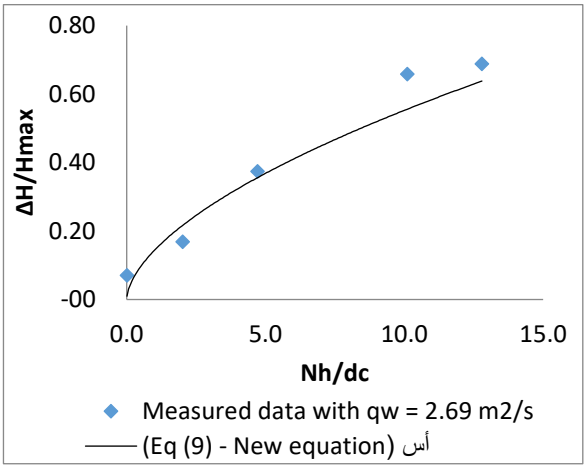

Figurre 14: ΔH/Hmax as a function of Nh/dc for qw = 2.69 m^2/s.

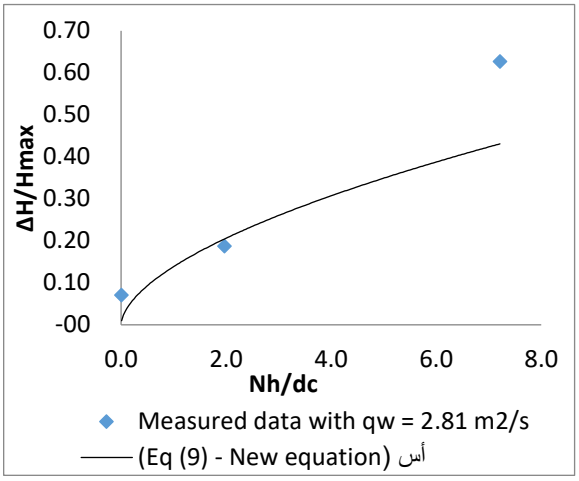

Figurre 15: ΔH/Hmax as a function of Nh/dc for qw = 2.81 m^2/s.

4. CONCLUSION

In both the nappe flow and skimming flow regimes, the measured data sets, in terms of energy dissipation, compared well with Eq (8) and Eq (9). The Pearson correlation for the nappe flow was 0.99 and for the skimming flow was between 0.97 and 0.99. For a given discharge, energy losses increase sharply with an increasing dam height, which is in line with [23, 24, 25, 26].

ACKNOWLEDGEMENTS

We acknowledge the fruitful discussions and contributions of Prof Hubert Chanson of the Department of Civil Engineering, The University of Queensland, Brisbane QLD 4072, Australia.

We also acknowledge the kind permission of Ruff and Ward (2002) to reproduce the measured data sets used in this study.

LIST OF SYMBOLS

The following symbols are used in this report:

C void fraction defined as the volume of air per unit volume of air and water; it is also called air concentration or local air content;

D_H hydraulic diameter (m);

d equivalent clear water flow depth (m);

dc critical flow depth (m): ;

g gravity constant (m/s^2);

H total head (m);

H_{dam} dam height (m);

H_{max} maximum upstream head (m) above chute toe:

$H_{max} = H_{dam} + 3/2 \times dc$;
H_{res} residual head (m);
h vertical step height (m);
l horizontal step length (m);
q_w water discharge per unit width (m^2/s);
Re Reynolds number defined in terms of the hydraulic diameter: $Re = \rho_w \times U_w \times D_H/\mu_w$;
U_w mean flow velocity (m/s): $U_w = q_w/d$;
U_w average mean flow velocity (m/s) for stepped spillway
W channel width (m);
Y_{90} characteristic depth (m) where the void fraction is 90%;
d distance (m) measured normal to the invert (or channel bed);
ΔH total head loss (m): $\Delta H = H_{max} - H_{res}$;
θ angle between pseudo-bottom formed by the step edges and the horizontal;

Subscript
c critical flow conditions;
max maximum value;
mean mean signal component;
w water properties;

REFERENCES

[1] G. Halbronn, R. Durand, G. Cohen de Lara, G., "Air Entrainment in Steeply Sloping Flumes", Proc. 5th IAHR Congress, IAHR-ASCE, Minneapolis, Usa, pp. 455–466, 1995.

[2] V. Jevdjevich, L. Levin, "Entrainment of air in flowing water and technical problems connected with it", In: Proc. 5th IAHR Congress. IAHR-ASCE, Minneapolis, Usa, pp. 439–454, 1953.

[3] H. Chanson,, "Air Bubble Entrainment in Free-Surface Turbulent Shear Flows," Academic Press, Lon-don, Uk, pp. 401-415, 1997 .

[4] N. S. L. Rao, and H. E.Kobus, "Characteristics of Self-Aerated Free-Surface Flows," Water and Waste Water/Current Research and Practice, Vol. 10, 1974.

[5] I. R. Wood, "Air entrainment in free-surface flows," In: IAHR Hydraulic Structures Design Manual No. 4, Hydraulic Design Considerations. Balkema Publ., Rotter-dam, The Netherlands, pp. 149, 1991.

[6] H. Kobus, "Local air entrainment and detrainment," In: Iahr, Esslingen, Germany, H., Kobus (Eds.), Proceedings International Symposium on Scale Effects in Modelling Hydraulic Structures, p. 10, Paper 4 – 10, 1984.

[7] H. Chanson, and C. Gualtieri,"Similitude and scale effects of air entrainment in hydraulic jumps," J. Hydraul. Res. IAHR, vol. 46, No. 1, pp. 35–44, 2008. doi:https://doi.org/10.1080/00221686.2008.9521841.

[8] I. R. Wood, "Air water flows," In: Proc. 21st IAHR Congress, IAHR, Melbourne, Australia, Keynote address, pp 18-29, 1985.

[9] H. Chanson, "Turbulent air-water flows in hydralic structures: dynamic similarity and scale effects," Environ. Fluid Mech., vol. 9, No. 2, pp. 125–142. doi:https://doi.org/10.1007/ s10652-008-9078-3, 2009.

[10] O. Ozueigbo and J. Agunwamba, "New Equations for Energy Dissipation down a Stepped Spillway, August 2022", Journal of Engineering Research and Reports (JERR), 2022, doi:https://doi.org/10.9734/jerr/2022/v23i417602.

[11] M .Hino, "On the mechanism of self-aerated flow on steep slope channels. Applications of the statistical theory of turbulence," 1961.

[12] P Dang, B. Nam, H.Quang, T.Huy, "Internal Energy Dissipator in Highway Steep Box Culverts - Effectiveness of Roughness Elements at the End Part of the Culverts", International Journal of Engineering Trends and Technology, vol. 70 No. 12, pp. 431-438, December, 2022, doi: https://doi.org/10.14445/22315381/IJETT-70I12P241

[13] H. Chanson,"Convective transport of air bubbles in strong hydraulic jumps", Int. J. Multiphase, Flow vol. 36, No. 10, pp. 798–814, 2010, doi: https://doi.org/10.1016/j.

[14] G. Gualtieri, and H. Chanson, "Effect of Froude number on bubble clustering in a hydraulic jump", J. Hydraul. Res. IAHR vol. 48, No. 4, pp. 504–508, Aug., 2010, doi: https://doi.org/10.1080/00221686.2010.491688.

[15] G. Gualtieri and H. Chanson, "Interparticle arrival time analysis of bubble distributions in a dropshaft and hydraulic jump", J. Hydraul. Res. IAHR, vol. 51, No. 3, pp. 253-264, June, 2013, doi: https://doi.org/10.1080/00221686.2012.762430.

[16] H. Wang and H. Chanson, "Self-similarity and scale effects in physical modelling of hydraulic jump roller dynamics, air entrainment and turbulent scales", Environ. Fluid Mech. vol. 16, No. 6, pp. 1087–1110, 2016, doi: https://doi.org/10.1007/s10652-016-9466-z.

[17] R. M. Boes, "Zweiphasenströmung und Energieumsetzung an Grosskaskaden," PhD thesis, VAW-ETH, Zürich, Switzerland (in German), 2000.

[18] G. Zhang and H. Chanson, "Effects of Step and Cavity Shapes on Aeration and Energy Dissipation Performances of Stepped Chutes", Journal of Hydraulic Engineering, ASCE, Vol. 144, No. 9, Paper 04018060, 2018, doi: https://doi: 10.1061/(ASCE)HY.1943-7900.0001505.

[19] H. Chanson and G. Carosi, "Advanced post-processing and correlation analyses in high-velocity air– water flows", Environ Fluid Mech, vol. 7, No. 6, pp. 495–508, 2007.

[20] S. Felder, "Air–water flow properties on stepped spillways for embankment dams: aeration, energy dissipation and turbulence on uniform, non-uniform and pooled stepped chutes", PhD Thesis, The University of

Queensland, Australia, 2013.
[21] L. Toombes, "Experimental study of air–water flow properties on low-gradient stepped cascades", PhD Thesis, Dept. of Civil Engineering, University of Queensland, Australia, 2002.
[22] H. Chanson, "The hydraulics of stepped chutes and spillways". Balkema, Lisse, pp 418-425, 2001.
[23] Chanson, H., "Air–water flow measurements with intrusive phase-detection probes. Can we improve their interpretation?" J Hydraul Eng ASCE, Vol. 128, No 3, pp. 252–255, 2002.
[24] H. Chanson, "Minimum specific energy and critical flow conditions in open channels", J Irrig Drain Eng ASCE, vol. 132, No 5, pp. 498–502, 2006.
[25] S. Felder, and H. Chanson, "Turbulence, dynamic similarity and scale effects in high-velocity freesurface flows above a stepped chute", Exp Fluids, vol. 47, No 1, pp. 1–18, 2009b.
[26] H. Chanson, and L. Toombes, "Air–water flows down stepped chutes: turbulence and flow structure observations", Int J Multiph Flow, vol. 28, No. 11, pp. 1737–1761, 2002a.